

Spatially Distributed Heterogeneous Limited Range Locational Optimization using Generalized Voronoi Partition

K.R. Guruprasad and Debasish Ghose

Abstract

In this paper a generalization of the Voronoi partition is used for solving a heterogeneous distributed locational optimization problem for autonomous agents, such as AGVs, UAVs, etc. The problem addressed is of optimal deployment of agents equipped with sensors, having heterogeneous capabilities, and limited range, to maximize sensor coverage. An objective function for optimal deployment of agents is formulated, and its critical points are determined. The optimal deployment is shown to be the generalized centroidal Voronoi configuration in which the agents are located at the centroids of the corresponding generalized Voronoi cells. Formal results on stability, convergence, and on spatial distribution of the proposed control laws responsible for agent motion, under some constraints on the agents' speeds and limit on sensor range are provided. The theoretical results are supported with illustrative simulation results.

Index Terms

Voronoi partition; Sensor Coverage; Locational Optimization; multi-agent system

K.R. Guruprasad is an Assistant Professor at the Department of Mechanical Engineering, National Institute of Technology Karnataka, Surathkal, 575025, India, and is currently working at the Department of Computer Science, University of Nebraska, Omaha, Nebraska, USA, as a visiting faculty. krgrprao@gmail.com (**Corresponding author**)

Debasish Ghose is a Professor at the Guidance, Control, and Decision Systems Laboratory, Department of Aerospace Engineering, Indian Institute of Science, Bangalore, 560012, India. dghose@aero.iisc.ernet.in

I. INTRODUCTION

A. *Multi-Agent Systems*

Technological advances in areas such as wireless communication, autonomous vehicular technology, computation, and sensors, facilitate the use of a large number of agents (UAVs, mobile robots, autonomous vehicles etc.), equipped with sensors, and with communication and computation ability, to cooperatively achieve various tasks in a distributed manner. Distributed multi-agent systems have been shown to achieve and maintain formations, move as flocks while avoiding obstacles, etc., thus mimicking their biological counterparts. They can also be used in applications such as search and rescue [3], surveillance[4], [5], target tracking[6], [7], [8], etc. The major advantages of distributed systems are substantial immunity to failure of individual agents, their versatility in accomplishing multiple tasks, simplicity of agents' hardware, and requirement of only minimal local information. However, it is important to design distributed control laws that guarantee stability and convergence to the desired collective behavior under limited information and evolving network configurations. One very useful application of the multi-agent systems is in sensor networks, where a group of autonomous agents perform cooperative sensing of a large geographical area. This paper addresses the problem of optimal deployment of autonomous agents equipped with sensors, communication equipment, and computational capability.

B. *Related Literature*

Cassandras and Li [9] provide an overview of sensor networks from a systems and control perspective. Li and Cassandras [10] represent frequency of occurrence of an event as a density function. The network model is probabilistic and assumes that the sensors make observations independently and maximize the expected event detection frequency, incorporating communication costs. Zou and Chakrabarty [11] use the concept of virtual force to solve a similar problem. Hussien and Stipanovic [12] address a problem of covering a compact domain using multiple agents such that each point is surveyed until a certain preset level is achieved using a centralized control law. Chakrabarty et al. [13] address a problem of placing sensors in a grid, based on the target distribution. Sensors have different range of detection, and those with higher detection range are assumed to have higher cost. Sensors are placed in such a way that every grid point is covered by a unique subset of sensors, so that the set of sensors reporting a target uniquely

identify the grid location for the target. They formulate the sensor placement problem in terms of cost minimization under coverage constraints, and then develop an integer programming (ILP) model to solve the sensor deployment problem. Murray et al. [14] address a problem of placing sensors such as video cameras for security monitoring. The problem is modeled using the maximal covering location problem (MCLP) and/or the backup coverage location problem (BCLP) combined with visibility analysis. Akbarzadeh et al. [15] address a sensor deployment problem using evolutionary algorithm approach. They also consider anisotropy in the sensors. Yao et al. [4] address a problem of camera placement for persistent surveillance, ensuring a sufficient uniform overlap between cameras' field of views to track a moving object.

One of the problems addressed in sensor networks literature is of optimally locating the sensors so as to maximize the measurement quality. This class of problems belongs to the problem of locational optimization or facility location [16], [17]. A centroidal Voronoi configuration is a standard solution for this class of problems when homogeneous sensors are used [18]. Voronoi decomposition or Dirichlet tessellation is a widely used partitioning scheme. It finds application in image processing, CAD, sensor coverage, multi-agent search [19], and several other areas. Salapaka et al. [20] address a pre-positioning problem of UAVs and the resources for anticipated response using deterministic annealing algorithm. Cortes et al. [21] address the problem of optimal deployment of sensors with limited range in a spatially distributed manner using Voronoi partition. A density distribution as a measure of the probability of occurrence of an event is used, along with a function of the Euclidean distance providing a quantitative assessment of the sensing performance, to formulate the problem. Centroidal Voronoi configuration, with centroids of Voronoi cells computed based on the density distribution within the cell, is shown to be the optimal deployment of sensors minimizing the sensory error. Cavalier et al. [22] address a problem of locating a finite number of sensors to detect an event in a given planar region. They use a heuristic based on Voronoi polygons to locate the sensors, where the objective is of minimizing the maximum probability of non-detection in a convex polygon. Pimenta et al. [23] follow an approach similar to [21] to address a problem with heterogeneous robots. The authors let the sensors be of different types (in the sense of having different footprints) and relax the point robot assumption. Power diagram (or Voronoi diagram in Laguerre geometry), a generalization of the standard Voronoi partition, is used to account for different footprints of the sensors. Due to the assumption of finite size of robots, the robots are assumed to be discs and

a free Voronoi region that excludes the robot footprints, is defined and a constrained locational optimization problem is solved. They also extend the results to non-convex environments. Kwok and Martínez [24] use power weighted and multiplicatively weighted Voronoi partitions to solve an energy aware limited range coverage problem. The energy content of the agents is used to determine the *power weights* or the *multiplicative weights*. The range of each agent is also a function of energy reserve, which reduces as the agents move. Pavone et al. [25] use power diagrams for solving problem of equitable partitioning for robotic networks. Unlike in a locational optimization problem, the agent location is fixed, and the partitioning is such that loads on all robots is uniform. A generalization of Voronoi partition is proposed in [26] to design optimal deployment strategy for agents having sensors with heterogeneous capabilities. The concept of node a function, instead of the usual distance measure in standard Voronoi partition, was introduced in this paper and sensor effectiveness functions were used as node functions.

In [27], the authors consider agents with sensors having anisotropic effectiveness, in the sense that effectiveness of the sensor at a point in space depends on the direction as well as the Euclidian distance from the sensor. They use Voronoi partition based on a non-Euclidian distance measure incorporating the anisotropy of sensors to solve the optimal sensor deployment problem. Laventall and Cortés [28] address a problem of multi-robot coverage control with limited-range anisotropic sensors. The sensor's footprint is a sector of circular disc with finite radius. They define a limited-range wedge proximity graph, where an agent is connected to another agent if the intersection of their Voronoi cells and its wedge shaped sensory region have a non-null intersection.

Zhong and Cassandras [29] address a problem of distributed coverage control of sensor networks in environments with polygonal obstacles. They use an event density function to capture the frequency of occurrence of random events in some point in the mission space. The mission space contains polygonal obstacles, whose configuration is known *a priori*. The probability that a sensor node detects an event occurring at a point in mission space is used as a sensing model, which is a monotonically decreasing function of the Euclidean distance. The function is assumed to be discontinuous in the position of the sensor due to the presence of obstacles. A gradient based control scheme is proposed to maximize (locally) the joint detection probability. Caicedo-núñez and Žefran [30] map a non-convex region, or a convex region with obstacles, into an almost convex region (in the sense of a finite set of points removed from a convex region) using

a diffeomorphism and then solve a convex coverage problem using Lloyd's algorithm.

C. Main contributions

In the literature, sensors in a network are usually considered to be homogeneous in their capability. Whereas, in practical problems, the sensors may have different capabilities even though they are similar in their functionality. The heterogeneity in capabilities could be due to various reasons, the chief being the difference in specified performance.

Some of the literatures address locational optimization of sensors which are heterogeneous [23], [25] and anisotropic [27], [28]. In such cases, a well known generalization of the standard Voronoi partition (weighted Voronoi partition, Power diagram, Voronoi diagram with non-Euclidean metric, etc.) is used to address the heterogeneity or anisotropy. These variations of Voronoi partitioning scheme can address heterogeneity of specific nature as evident from the literature.

This paper generalizes the standard Voronoi partition to address a class of heterogeneous locational optimization problems, which include some of the problems addressed in the literature. A concept of node functions is introduced in the place of the usual distance measure used in standard Voronoi partition and its variants. The mobile sensors are assumed to have heterogeneous capabilities in terms of their effectiveness. A density distribution is used as a measure of probability of occurrence of an event of interest. It is shown that the optimal deployment configuration is the generalized centroidal Voronoi configuration. A proportional control law is proposed to make the sensors move toward the optimal configuration. Assuming first order dynamics for the mobile sensors, it is proved, using LaSalle's invariance principle, that the trajectories of the sensors converge to the optimal configuration globally and asymptotically. Further, the problem is analyzed in the presence of some constraints on the agents' speeds and with limit on its sensor range. Some preliminary results on heterogeneous limited range locational optimization problem have been reported in [26] earlier. This paper gives a more elaborate treatment with several new results.

This paper addresses a problem of locational optimization for sensors whose effectiveness is assumed to be strictly decreasing functions of the Euclidean distance between the sensor location and a point of interest. This is in contrast with the work of Kwok and Martínez [24] which addresses an energy aware limited range coverage problem, and uses one of the well known

generalization of the standard Voronoi partition namely, the multiplicatively weighted Voronoi partition to solve the problem, with the multiplicative weight being related to the energy content of the robots which decrease as they move.

This paper focuses on sensor coverage problem in a convex domain. However, each generalized Voronoi cell can be non-convex. Some of the work on coverage in non-convex domain have been reported in the literature [29], [30], which can be used for extending the present work to non-convex domain.

D. Organization of the paper

A generalization of the Voronoi partition is discussed in Section II. Section III introduces the heterogeneous locational optimization problem along with the objective function, its critical points, the control law and its properties. In Section IV the problem is analyzed with some constraints on the speed of the agents. The sensor range limits are considered and the limited range distributed heterogeneous locational optimization problem is addressed in Section V. Section VI provides simulation results and the paper is concluded in Section VII with some discussions on scope for future work.

II. GENERALIZATION OF THE VORONOI PARTITION

Voronoi partition [31], [32] is a widely used scheme of partitioning a given space and finds applications in many fields such as CAD, image processing and sensor coverage. The standard Voronoi partition is briefly previewed and a generalized Voronoi partition used in this work is presented.

A. Standard Voronoi partition

Let $I_N = \{1, 2, \dots, N\}$. A collection $\mathcal{W} = \{W_i\}$, $i \in I_N$ of subsets of a space X with disjoint interiors is said to be a partition of X if $\cup_{i \in I_N} W_i = X$.

Let $Q \subset \mathbb{R}^d$, be a convex polytope in d -dimension Euclidean space. Let \mathcal{P} be the set of nodes or generators in Q . The *Voronoi partition* generated by \mathcal{P} with respect to the Euclidean norm is the collection $\mathcal{V}(\mathcal{P}) = \{V_i(\mathcal{P})\}_{i \in I_N}$, and is defined as,

$$V_i(\mathcal{P}) = \{q \in Q \mid \|q - p_i\| \leq \|q - p_j\|, \forall p_j \in \mathcal{P}, j \in I_N\} \quad (1)$$

where, $\| \cdot \|$ denotes the Euclidean norm.

The Voronoi cell V_i is the collection of those points which are closest (with respect to the Euclidean metric) to p_i compared to any other point in \mathcal{P} . The boundary of each Voronoi cell is the union of a finite number of line segments forming a closed C^0 curve. In \mathbb{R}^2 , the intersection of any two Voronoi cells is either null, a line segment, or a point. In d dimensional space, the boundaries of the Voronoi cells are unions of convex subsets of at most $d - 1$ dimensional hyperplanes in \mathbb{R}^d and the intersection of two Voronoi cells is either a convex subset of a hyperplane or a null set. Each of the Voronoi cells is a topologically connected non-null set.

The basic components of the Voronoi partition are: i) A space to be partitioned; ii) A set of sites, or nodes, or generators; and iii) A distance measure such as the Euclidean distance.

B. Generalization of Voronoi partition

A generalization of the Voronoi partition, considering heterogeneity in the sensors' capabilities, is presented here. Several extensions or generalizations of Voronoi partition to suit specific applications have been reported in the literature [17], [33], [34]. Herbert and Seidel [35] have introduced an approach in which, instead of the site set, a finite set of real-valued functions $f_i : D \mapsto \mathbb{R}$ is used to partition the domain D . Standard Voronoi partition and other known generalizations can be extracted from this abstract general form.

In this paper a generalization of the Voronoi partition is defined to suit the application, namely the heterogeneous locational optimization of sensors. This generalization has the following components: i) The domain of interest as the space to be partitioned; ii) The configuration of multi-agent system \mathcal{P} as the site (or node or generator) set; and iii) A set of node functions in place of a distance measure.

Consider a space $Q \subset \mathbb{R}^d$, a set of points called *nodes* or *generators* $\mathcal{P} = \{p_1, p_2, \dots, p_N\}$, $p_i \in Q$, with $p_i \neq p_j$, whenever $i \neq j$, and strictly decreasing analytic functions $f_i : \mathbb{R}^+ \mapsto \mathbb{R}$, where, f_i is called a *node function* for the i -th node. Define *generalized Voronoi partition* of Q with node configuration \mathcal{P} and node functions f_i as a collection $\mathcal{V}^g = \{V_i^g\}$, $i \in I_N$, with mutually disjoint interiors, such that $Q = \cup_{i \in I_N} V_i^g$, where V_i^g is defined as

$$V_i^g = \{q \in Q | f_i(\|p_i - q\|) \geq f_j(\|p_j - q\|), \quad \forall j \neq i, j \in I_N\} \quad (2)$$

Note that: V_i^g can be topologically non-connected, null, and may contain other Voronoi cells; In the context of the problem discussed in this paper, $q \in V_i^g$ means that the i -th agent/sensor

is the most effective in sensing at point q . This is reflected in the \geq sign in the definition. In standard Voronoi partition used for the homogeneous case, \leq sign for distances ensured that the i -th sensor is the most effective in V_i . (Note that f_i are strictly decreasing.); The condition that f_i are analytic implies that for every $i, j \in I_N$, $f_i - f_j$ is analytic. By the property of real analytic functions [36], the set of intersection points between any two node functions is a set of measure zero. This ensures that the intersection of any two cells is a set of measure zero, that is, the boundary of a cell is made up of the union of at most $d - 1$ dimensional subsets of \mathbb{R}^d . Otherwise the requirement that the cells should have mutually disjoint interiors may be violated. Analyticity of the node functions f_i is a sufficient condition to discount this possibility.

C. Special cases

The name ‘generalized Voronoi partition’ suggests that by suitably selecting parameters like the node functions, one should get the standard Voronoi partition and its generalizations as special cases. A few interesting special cases are discussed below.

Case 1: Weighted Voronoi partition: Consider multiplicatively and additively weighted Voronoi partitions as special cases. Let $f_i(r_i) = -\alpha_i r_i - d_i$ where, $r_i = \|p_i - q\|$ and, α_i and d_i take finite positive real values for $i \in I_N$. Thus,

$$V_i^w = \{q \in Q | \alpha_i r_i + d_i \leq \alpha_j r_j + d_j, \quad \forall j \neq i, \quad j \in I_N\} \quad (3)$$

The partition $\mathcal{V}^w = \{V_i^w\}$ is called a multiplicatively and additively weighted Voronoi partition. α_i are called multiplicative weights and d_i are called additive weights. With this generalization, Voronoi cells no longer possess the nice property of being topologically connected sets. The Voronoi cells could be made up of disjoint patches and one or more Voronoi cells can get embedded inside another cell.

Case 2: Standard Voronoi partition: The standard Voronoi partition can be obtained as a special case of (2) when the node functions are $f_i(r_i) = -r_i$. It can be shown that if the node functions are homogeneous ($f_i(\cdot) = f(\cdot)$ for each $i \in I_N$), then the generalized Voronoi partition gives the standard Voronoi partition.

Case 3: Power diagram: Power diagram or Voronoi diagram in Laguerre geometry $\mathcal{V}^{LG} = \{V_i^{LG}\}$ used in [23] is defined as $V_i^{LG} = \{q \in Q | d_p(q, p_i) \leq d_p(q, p_j), i \neq j\}, i, j \in I_N$ where, $d_p(q, p_i) = \|p_i - q\|^2 - R_{p_i}^2$, the power distance between q and p_i , with $R_{p_i} > 0$ being a parameter

fixed for a given node p_i . In the context of robot coverage problem addressed in [23], R_{P_i} represents the radius of the footprint of the i -th robot. It is easy to see that the power diagram can be obtained from the generalized Voronoi partition (2) by setting $f_i(\|q - p_i\|) = -(\|p_i - q\|^2 - R_{P_i}^2)$ with R_{P_i} as a parameter specific to each node function.

Case 4: Voronoi partition based on Non-Euclidean distance: One of the ways in which a standard Voronoi partition can be generalized is by using non-Euclidean distance. The distance measure used depends on the application. As an example, in [27], a non-Euclidean distance measure is used to incorporate anisotropy in sensor effectiveness. They define $d(q, p_i) = \|p_i - q\|_{L_i}$, with $\|p_i - q\|_{L_i} = (q - p_i)^T L_i (q - p_i)$, where $L_i = F_i^T F_i$ with

$$F_i = \left[\begin{pmatrix} c/a & 0 \\ 0 & c/b \end{pmatrix} \begin{pmatrix} \cos \theta_i & \sin \theta_i \\ -\sin \theta_i & \cos \theta_i \end{pmatrix} \right]$$

By setting the node function as $f_i(\|p_i - q\|_{L_i}) = -\|p_i - q\|_{L_i}$, in the generalized Voronoi partition (2), the generalization of Voronoi diagram used in [27] can be obtained.

Case 5: Other possible variations: Other possible variations of the Voronoi partition are using objects such as lines, curves, discs, polytopes, etc. other than points as sites/nodes, generalization of the space to be partitioned, and use of non-Euclidean metrics or pseudo-metrics. It is easy to verify that these generalizations can also be obtained by suitable selection of site sets, spaces, and node functions.

D. Generalized Delaunay graph

Delaunay graph is the dual of Voronoi partition. Two nodes are said to be neighbors (connected by an edge), if the corresponding Voronoi cells are adjacent. This concept can be extended to generalized Voronoi partitioning scheme. Note that the *generalized Delaunay graph*, \mathcal{G}_D^g , in general, need not have the property of Delaunay triangulation, in fact, it need not even be a triangulation. Two nodes are said to be neighbors in \mathcal{G}_D^g , if the corresponding generalized Voronoi cells are adjacent. The set of neighbors of a node i is defined as $N_{\mathcal{G}_D^g} = \{j | V_i^g \cap V_j^g \neq \emptyset, i \neq j \in I_N\}$.

E. Centroid of a generalized Voronoi cell

A result on the location of centroid of a generalized Voronoi cell which will be used later in the paper is discussed here.

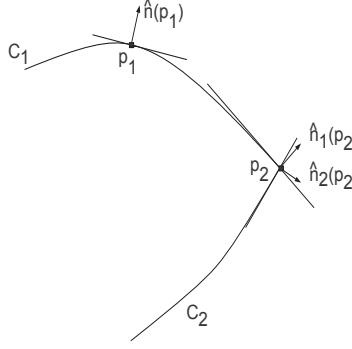


Fig. 1. Illustration of centroid of a convex set

Lemma 1: Let $W \subset \mathbb{R}^d$ be a closed convex set. Then centroid $C_W \in W$.

Proof. Let $W \subset \mathbb{R}^d$ be a convex set, and $\phi(q)$ be the density at $q \in W$. The centroid of W is given by,

$$C_W = \frac{\int_W \phi(q) q dQ}{\int_W \phi(q) dQ} \quad (4)$$

Let p be any point in ∂W , the boundary of W , and $\hat{n}(p)$ is the unit outward normal to W at $p \in \partial W$. Then,

$$\hat{n}(p) \cdot (C_W - p) = \frac{\int_W \phi(q) \hat{n}(p) \cdot (q - p) dQ}{\int_W \phi(q) dQ} \quad (5)$$

Note that the quantity $\hat{n}(p) \cdot (q - p) \leq 0$, $\forall q \in W$. (Equality holds only when q is on L , the hyperplane tangential to ∂W at p . The set $L \cap W$ is either a convex subset of L or is the singleton $\{q = p\}$.) Thus, $\hat{n}(p) \cdot (C_W - p) \leq 0$. This is true for all $p \in \partial W$. Thus, $C_W \in W$. \square

Corollary 1: The centroid of a closed subset of \mathbb{R}^d is within its convex hull.

Proof Let $W \subset \mathbb{R}^d$, and let $\text{co}(W)$ be the convex hull of W . The centroid of W is given by,

$$C_W = \frac{\int_W \phi(q) q dQ}{\int_W \phi(q) dQ} = \frac{\int_{\text{co}(W)} \phi(q) q dQ}{\int_{\text{co}(W)} \phi(q) dQ} = C_{\text{co}(W)} \quad (6)$$

with $\phi(q) = 0, \forall q \in \text{co}(W) \setminus W$. By Lemma 1, $C_W \in \text{co}(W)$. \square

Theorem 1: The centroid of a generalized Voronoi cell will be in its convex hull.

The proof follows from Corollary 1. \square

III. HETEROGENEOUS LOCATIONAL OPTIMIZATION PROBLEM

The heterogeneous locational optimization problem (HLOP) for a mobile sensor network is formulated and solved here. Let $Q \subset \mathbb{R}^d$ be a convex polytope, the space in which the

sensors have to be deployed; $\phi : Q \mapsto [0, 1]$, be a density distribution function; $\mathcal{P}(t) = \{p_1(t), p_2(t), \dots, p_N(t)\}, i \in I_N, p_i(t) \in Q$ be the configuration of N sensors at time t ; $f_i : \mathbb{R}^+ \mapsto \mathbb{R}, i \in I_N$, be analytic, strictly decreasing function corresponding to the i -th node, the sensor effectiveness function of i -th agent; and $V_i^g \subset Q$ be the generalized Voronoi cell corresponding to the i -th node/sensor.

The density $\phi(q)$ is the probability of an event of interest occurring in $q \in Q$, indicating the importance of measurement at the given point in Q . As $\phi(q) \rightarrow 1$, the importance of measurement at q increases as the probability of occurrence of an event of interest is higher. The objective of the problem is to deploy the sensors in Q so as to maximize the probability of detection of an event of interest. Let f_i be a function of the Euclidean distance of a point of interest $q \in Q$ from the location of the i -th sensor p_i , indicating the effectiveness of sensing. It is natural to assume f_i to be strictly decreasing.

In case of homogeneous sensors, the sensor located in Voronoi cell V_i is closest to all the points $q \in V_i$ and hence, by the strictly decreasing variation of sensor's effectiveness with distance, the sensor is most effective within V_i . Thus, the Voronoi decomposition leads to optimal partitioning of the space in the sense that each sensor is most effective within its Voronoi cell. In the heterogeneous case too, it is easy to see that each sensor is most effective in its own generalized Voronoi cell, by the very definition of the generalized Voronoi decomposition. Now, as the partitioning is optimal, the problem is to find the location of each sensor within its generalized Voronoi cell.

A. The objective function

Consider the following objective function to be maximized,

$$\mathcal{H}(\mathcal{P}) = \int_Q \max_{i \in I_N} \{f_i(\|q - p_i\|)\} \phi(q) dQ = \sum_{i \in I_N} \int_{V_i^g} f_i(\|q - p_i\|) \phi(q) dQ \quad (7)$$

where, $\|\cdot\|$ is the Euclidean distance. Note that the generalized Voronoi decomposition splits the objective function into a sum of contributions from each generalized Voronoi cell. Hence the optimization problem can be solved in a spatially distributed manner, that is, the optimal configuration can be achieved by each sensor solving only that part of the objective function which corresponds to its own cell, using only local information.

Lemma 2: The gradient of the objective function (7) with respect to p_i is

$$\frac{\partial \mathcal{H}}{\partial p_i} = \int_{V_i^g} \phi(q) \frac{\partial f_i(r_i)}{\partial p_i} dQ \quad (8)$$

Proof. Applying the general form of the Leibniz theorem [37]

$$\begin{aligned} \frac{\partial \mathcal{H}}{\partial p_i} &= \int_{V_i^g} \phi(q) \frac{\partial f_i(r_i)}{\partial p_i} dQ + \sum_{j \in N_{\mathcal{G}_D^g}(i)} \int_{A_{ij}} \mathbf{n}_{ij}(q) \cdot \mathbf{u}_{ij}(q) \phi(q) f_i(r_i) dQ \\ &\quad + \sum_{j \in N_{\mathcal{G}_D^g}(i)} \int_{A_{ji}} \mathbf{n}_{ji}(q) \cdot \mathbf{u}_{ji}(q) \phi(q) f_j(r_j) dQ \end{aligned} \quad (9)$$

where, A_{ij} is the bounding surface (hyper-plane) common to V_i^g and V_j^g , $\mathbf{n}_{ij}(q)$ is the unit outward normal to A_{ij} at $q \in A_{ij}$, $\mathbf{u}_{ij}(q) = \frac{dA_{ij}}{dp_i}(q)$, the rate of movement of the boundary at $q \in A_{ij}$ with respect to p_i . Note that $\mathbf{u}_{ij}(q) = \mathbf{u}_{ji}(q)$, $\mathbf{n}_{ij}(q) = -\mathbf{n}_{ji}(q)$, $f_i(r_i) = f_j(r_j)$, $\forall q \in A_{ij}$ (by definition of the generalized Voronoi partition), and ϕ is bounded. Thus the last two terms in right-hand side of (9) cancel out. \square

B. The critical points

The gradient of the objective function (7) with respect to p_i , the location of the i -th node in Q , can be determined using (8) (by Lemma 2) as

$$\frac{\partial \mathcal{H}}{\partial p_i} = \int_{V_i^g} \phi(q) \frac{\partial f_i(r_i)}{\partial p_i} dQ = - \int_{V_i^g} \tilde{\phi}^i(q, p_i) (p_i - q) dQ = -\tilde{M}_{V_i^g} (p_i - \tilde{C}_{V_i^g}) \quad (10)$$

where, $\tilde{\phi}^i(q, p_i) = -2\phi(q) \frac{\partial f_i(r_i)}{\partial (r_i^2)}$. As f_i s are strictly decreasing, $\tilde{\phi}(q)$ is always non-negative. Hence, $\tilde{\phi}$ can be interpreted as density modified or perceived by the sensors, $\tilde{M}_{V_i^g}$ as mass, and $\tilde{C}_{V_i^g}$ as centroid of the cell V_i^g . Thus, the critical points/configurations are $\mathcal{P}^* = \{\mathcal{P} | p_i = \tilde{C}_{V_i^g}(\mathcal{P}), i \in I_N\}$, and such a configuration \mathcal{P}^* , of agents is called a *generalized centroidal Voronoi configuration*.

Theorem 2: The gradient, given by (10), is spatially distributed over the *generalized Delaunay graph* \mathcal{G}_D^g .

Proof. The gradient (10) with respect to $p_i \in \mathcal{P}$, the present configuration, depends only on the corresponding generalized Voronoi cell V_i^g and values of $\phi(q)$, $q \in V_i^g$ and the gradient of f_i . The generalized Voronoi cell V_i^g depends only on the neighbors $N_{\mathcal{G}_D^g(\mathcal{P})}(i)$ of i . Thus, the gradient (10) can be computed with only local information. \square

The critical points are not unique, as with the standard Voronoi partition. But in the case of a generalized Voronoi partition, some of the cells could become null and such a condition can lead to local minima.

C. The control law

Consider the sensor dynamics and control law as

$$\dot{p}_i(t) = u_i(t) \quad (11)$$

$$u_i(t) = -k_{prop}(p_i(t) - \tilde{C}_{V_i^g}(t)) \quad (12)$$

Control law (12) makes the mobile sensors move toward $\tilde{C}_{V_i^g}$ for positive k_{prop} . If, for some $i \in I_N$, $V_i^g = \emptyset$, then set $\tilde{C}_{V_i^g} = p_i$. We restrict the analysis to the simple first order dynamics under the assumption, that there is a low-level controller which can cancel the actual dynamics of the agents and enforce (11). The control law (12) can be computed in a spatially distributed manner in \mathcal{G}_D^g as it is based on the gradient (10) which is a spatially distributed function on \mathcal{G}_D^g by the Theorem 2.

Theorem 3: The trajectories of the sensors governed by the control law (12), starting from any initial condition $\mathcal{P}(0)$, will asymptotically converge to the critical points of \mathcal{H} .

Proof. Here LaSalle's invariance principle is used. Important differences of the LaSalle's invariance principle as compared to the Lyapunov Theorem are (i) \dot{V} is required to be negative semi-definite rather than negative definite and (ii) the function V need not be positive definite (see Remark on Theorem 3.8 in [38], pp 90-91). Consider $V(\mathcal{P}) = -\mathcal{H}$.

$$\dot{V}(\mathcal{P}) = -\frac{d\mathcal{H}}{dt} = -\sum_{i \in I_N} \frac{\partial \mathcal{H}}{\partial p_i} \dot{p}_i = -k_{prop} \sum_{i \in I_N} \tilde{M}_{V_i^g} (p_i - \tilde{C}_{V_i^g})^2 \quad (13)$$

Let $p_i \in \partial Q$, the boundary of Q for some i at some time t . The vector $\dot{p}_i = -k_{prop}(p_i - \tilde{C}_{V_i^g})$ always points inward to Q or is tangential to ∂Q at p_i as $\tilde{C}_{V_i^g} \in Q$ by Theorem 1 (Note that $\text{co}(V_i^g) \subset Q$). Thus, by Theorem 3.1 in [39], the set Q is invariant under the closed-loop dynamics given by (11) and (12).

Further, observe that, $V : Q \mapsto \mathbb{R}$ is continuously differentiable in Q as $\{V_i\}$ depends continuously on \mathcal{P} by Theorem A1 (see Appendix); Q is a compact invariant set; \dot{V} is negative semi-definite in Q ; $E = \dot{V}^{-1}(0) = \{\tilde{C}_{V_i^g}\}$, which itself is the largest invariant subset of E by the control law (12). Thus by LaSalle's invariance principle, the trajectories of the agents

governed by control law (12), starting from any initial configuration $\mathcal{P}(0)$ (Note by definition, $p_i(0) \in Q, \forall i \in I_N$), will asymptotically converge to set E , the critical points of \mathcal{H} , that is, the centroids of the generalized centroidal Voronoi cells with respect to the density function as perceived by the sensors. \square

IV. CONSTRAINTS ON AGENTS' SPEEDS

The proposed control law (12) guides the agents toward the critical points, that is, toward the centroids of the respective generalized Voronoi cells, and it was observed that the closed loop system for agents, modeled as first order dynamical system, is globally asymptotically stable. Here, some constraints on the agent speeds are imposed and the dynamics of closed loop system will be analyzed.

A. Maximum speed constraint

Let the agents have a constraint on maximum speed of $U_{maxi} > 0$, for $i \in I_N$. Now, consider the control law

$$u_i = \begin{cases} -k_{prop}(p_i - \tilde{C}_{V_i}), & \text{If } \|k_{prop}(p_i - \tilde{C}_{V_i})\| \leq U_{maxi} \\ -U_{maxi} \frac{(p_i - \tilde{C}_{V_i})}{\|(p_i - \tilde{C}_{V_i})\|} & \text{Otherwise} \end{cases} \quad (14)$$

The control law (14) makes the agents move toward centroids of respective generalized Voronoi cells with a saturation on speed.

Similar to the control law (12), the control law (14) too is spatially distributed in \mathcal{G}_D^g .

Theorem 4: The trajectories of the agents governed by the control law (14), starting from any initial condition $\mathcal{P}(0) \in Q^N$, will asymptotically converge to the critical points of \mathcal{H} .

Proof. Consider $V(\mathcal{P}) = -\mathcal{H}$.

$$\dot{V}(\mathcal{P}) = -\sum_i^N \frac{\partial \mathcal{H}}{\partial p_i} \dot{p}_i = \begin{cases} -k_{prop} \sum_i^N \tilde{M}_{V_i^g} (\|p_i - \tilde{C}_{V_i^g}\|)^2, & \text{if } \|k_{prop}(p_i - \tilde{C}_{V_i^g})\| \leq U_{maxi} \\ -\sum_i^N U_{maxi} \tilde{M}_{V_i^g} \frac{(\|p_i - \tilde{C}_{V_i^g}\|)^2}{(\|p_i - \tilde{C}_{V_i^g}\|)}, & \text{otherwise} \end{cases} \quad (15)$$

It can be shown by similar arguments as in the proof of Theorem 3, that Q is invariant under the closed-loop dynamics given by (11) and (14).

Observe that $V : Q \mapsto \mathbb{R}$ is continuously differentiable in Q as $\{V_i\}$ depends at least continuously on \mathcal{P} (Theorem A3 given in Appendix), and \dot{V} is continuous as u is continuous;

$M = Q$ is a compact invariant set (see argument in the proof of Theorem 3); \dot{V} is negative semi-definite in M ; $E = \dot{V}^{-1}(0) = \{\tilde{C}_{V_i^g}\}$, which itself is the largest invariant subset of E by the control law (14). Thus, by LaSalle's invariance principle, the trajectories of the agents governed by control law (14), starting from any initial configuration $\mathcal{P}(0)$, will asymptotically converge to the set E , the critical points of \mathcal{H} , that is, the generalized centroidal Voronoi configuration with respect to the density as perceived by the sensors. \square

B. Constant speed control

The agents may have a constraint of moving with a constant speed U_i . The agents slow down as they approach the critical points. For $i \in I_N$, consider the control law

$$u_i = \begin{cases} -U_i \frac{(p_i - \tilde{C}_{V_i})}{\|p_i - \tilde{C}_{V_i}\|}, & \text{if } \|p_i - \tilde{C}_{V_i}\| \geq \delta \\ -U_i(p_i - \tilde{C}_{V_i})/\delta, & \text{otherwise} \end{cases} \quad (16)$$

where, $\delta > 0$, predefined value, such that the control law (16) makes the agents move toward their respective centroids with a constant speed of U_i when they are at a distance greater than δ from the corresponding centroids and slow down as they approach them. This case is similar to the case when agents have a limit on the maximum speed discussed earlier.

V. LIMITED RANGE SENSORS

In the previous sections, it was assumed that the sensors have infinite range but with diminishing effectiveness. However, in reality the sensors will have limited range. In this section a spatially distributed limited range locational optimization problem is formulated.

Let R_i be the limit on range of the sensors and $\bar{B}(p_i, R_i)$ be a closed ball centered at p_i with a radius of R_i . The i -th sensor has access to information only from points in the set $V_i^g \cap \bar{B}(p_i, R_i)$. Consider \hat{f}_i which is continuously differentiable in $[0, R_i]$, with $\hat{f}_i(R_i) = 0$, and $\hat{f}_i(r) = 0, \forall r > R_i$ as the sensor effectiveness function. This function models the effectiveness of a sensor having a limit of R_i on its range. Note that the derivative of \hat{f}_i can have a discontinuity at $r = R_i^+$, where $R_i^+ = \lim_{h \rightarrow 0}(R_i + h)$. Consider the following objective function to be maximized,

$$\hat{\mathcal{H}}(\mathcal{P}) = \sum_{i \in I_N} \int_{(V_i^g \cap \bar{B}(p_i, R_i))} \phi_n(q) \hat{f}_i(\|p_i - q\|) dQ \quad (17)$$

It can be noted that the objective function is made up of sums of the contributions from sets $V_i^g \cap \bar{B}(p_i, R_i)$, enabling the sensors to solve the optimization problem in a spatially distributed manner.

Lemma 3: The gradient of the multi-center objective function (17) with respect to p_i is given by

$$\frac{\partial \hat{\mathcal{H}}}{\partial p_i} = \int_{(V_i^g \cap \bar{B}(p_i, R_i))} \phi_n(q) \frac{\partial}{\partial p_i} \hat{f}_i(\|p_i - q\|) dQ \quad (18)$$

Proof. The boundary of $(V_i^g \cap \bar{B}(p_i, R_i))$ is made up of a collection of a few subsets of hypersurfaces (common boundary between neighboring Voronoi cells) and convex subsets of surface of a hypersphere (corresponding to $\bar{B}(p_i, R_i)$). Using similar arguments as in the proof of Lemma 2, it can be shown that the contributions from surface integrals over surfaces which are common boundaries between neighboring generalized Voronoi cells cancel out. Along the curved hypersurfaces (circular arcs in \mathbb{R}^2), $\hat{f}_i(r_i) = 0$ as $r_i = R_i$. Thus, the surface integral is identically zero. \square

Using Lemma 3, the gradient of the objective function (17) can be shown to be,

$$\frac{\partial \hat{\mathcal{H}}(\mathcal{P})}{\partial p_i} = -\tilde{M}_{(V_i^g \cap \bar{B}(p_i, R_i))} (p_i - \tilde{C}_{(V_i^g \cap \bar{B}(p_i, R_i))}) \quad (19)$$

where, the mass \tilde{M} and the centroid $\tilde{C}_{(V_i^g \cap \bar{B}(p_i, R_i))}$ are now computed within the region $(V_i^g \cap \bar{B}(p_i, R_i))$, that is, the region of Voronoi cell V_i^g , which is accessible to the i -th robot. The critical points/configurations are $\mathcal{P}^* = \{\mathcal{P} | p_i = \tilde{C}_{(V_i^g \cap \bar{B}(p_i, R_i))}(\mathcal{P}), i \in I_N\}$.

Consider the following control law to guide the agents toward the respective centroids

$$u_i = -k_{prop}(p_i - \tilde{C}_{(V_i^g \cap \bar{B}(p_i, R_i))}) \quad (20)$$

It can be observed, that the gradient (19) and hence the control law (20) can be computed by each agent in a spatially distributed manner in the r -limited generalized Delaunay graph \mathcal{G}_{LD}^g , the generalized Delaunay graph incorporating sensor range limits.

Theorem 5: The trajectories of the sensors governed by the control law (20), starting from any initial condition $\mathcal{P}(0)$, will asymptotically converge to the critical points of $\tilde{\mathcal{H}}$.

Proof. The proof is based on LaSalle's Theorem with $V = -\hat{\mathcal{H}}(\mathcal{P})$. The functions \hat{f}_i are continuous and ϕ is bounded. Further, the collection $\{(V_i^g \cap \bar{B}(p_i, R_i))\}$ can be shown to be continuous in \mathcal{P} . Further, \hat{f}_i are continuously differentiable almost everywhere and continuously

differentiable in $(V_i^g \cap \bar{B}(p_i, R_i))$, and hence, $\frac{\partial \hat{\mathcal{H}}(\mathcal{P})}{\partial p_i}$ is continuous. Now, \dot{V} is continuous as $\frac{\partial \hat{\mathcal{H}}(\mathcal{P})}{\partial p_i}$ and u_i are continuous $\forall i \in I_N$.

Suppose the i -th agent is located on ∂Q , the boundary of Q , at some time t . Let $L = \partial Q \cap (V_i^g \cap \bar{B}(p_i, R_i))$ be the part of a bounding hyperplane common to ∂Q and $(V_i^g \cap \bar{B}(p_i, R_i))$ and contains p_i , and let \hat{n} be its unit outward normal to L . From (11) and (20),

$$\dot{p}_i = -k_{prop}(p_i - \tilde{C}_{V_i^g \cap \bar{B}(p_i, R_i)}) = \frac{k_{prop}}{M_{(V_i^g \cap \bar{B}(p_i, R_i))}} \int_{V_i^g \cap \bar{B}(p_i, R_i)} \tilde{\phi}(q)(q - p_i) dQ \quad (21)$$

The inner product of \dot{p}_i with \hat{n} is given by,

$$\hat{n} \cdot \dot{p}_i = k_{prop} \frac{\int_{V_i^g \cap \bar{B}(p_i, R_i)} \tilde{\phi}(q) \hat{n} \cdot (q - p_i) dQ}{\int_{V_i^g \cap \bar{B}(p_i, R_i)} \tilde{\phi}(q) dQ}$$

Note that the quantity $\hat{n} \cdot (q - p_i) \leq 0$ (equality holds only for $q \in L$), and hence, $\hat{n} \cdot \dot{p}_i \leq 0$. That is \dot{p}_i points towards $\text{int}(Q)$, the interior of Q , or is tangential to it. Thus, by Theorem 3.1 in [39], Q is invariant under (21). The proof also follows as $\tilde{C}_{V_i^g \cap \bar{B}(p_i, R_i)} \in \text{co}(V_i^g \cap \bar{B}(p_i, R_i)) \in Q$. Rest of the proof is similar to that of Theorem 4. \square

VI. SIMULATION EXPERIMENTS

In this section an optimal deployment strategy is proposed based on the results obtained in this paper and a set of simulation experiments are given to validate the performance.

One of the drawbacks of Voronoi based deployment schemes is that of computational overhead. In order to make the deployment strategy proposed in this paper implementable in real situations, the space is discretized into cells. Hexagonal cells are preferred over square or rectangular cells because of the fact that in hexagonal grids all the neighboring cells are at equal distance. The space is partitioned into hexagonal cells, and the continuous space is approximated by the centers of cells. Now the generalized Voronoi cell is a set of hexagonal cells. This cellular structure simplifies the computations related to generalized Voronoi partition. The computation of centroid is also less intensive. The agents can occupy only the centers of hexagonal cells and the centroids are also approximated to the center of the cells. If a centroid falls in a cell indexed (i, j) , then the centroid is approximated as the center of that cell. We have considered two sets of node functions, i) $f_i(r_i) = -\alpha_i r_i^2$, and ii) $f_i(r_i) = k_i e^{-\alpha_i r_i^2}$. The first set leads to multiplicatively weighted Voronoi partition when $\alpha_i \neq \alpha_j$, for $i \neq j$. For any given set of node functions, three density distributions have been used: i) a uniform density, ii) an exponential density distribution

$\phi(x, y) = 0.9e^{-0.001((x-42)^2+(y-36)^2)}$ having a peak near the center of space, and iii) an exponential density distribution $\phi(x, y) = 0.9e^{-0.001((x-70)^2+(y-60)^2)}$ having peak toward the corner of the space. The space considered is a rectangular area with x-axis range 0-86 units and y-axis range 0-74 units. The optimal deployment is achieved when each of the agents are located at the respective centroids. Each hexagonal cell measures 1 unit from center to any of its corners.

Figure 2(a) shows the trajectories of $N = 10$ agents with $f_i(r_i) = -\alpha_i r_i^2$ and uniform density distribution. The actual generalized Voronoi partition corresponding to position of agents at the end of the deployment is also shown. The starting location of the agents are shown with dots and final positions with 'o's. The value of the parameter α corresponding to each agent is indicated near its final position. It can be observed that the agents spread out to cover the space. Agents having higher range, that is, agents having lower value of α , cover more space, which is indicated by larger generalized Voronoi cell. Figure 2(b) shows the corresponding results for homogeneous agents, that is $\alpha_i = \alpha_j$, for all $i, j \in I_N$. The corresponding generalized Voronoi partition is the same as the standard Voronoi partition. Note that the generalized Voronoi partitions shown in the all figures are only representative in the sense that they are not based on the hexagonal grids.

A normalized error measure of how close the agents are to the centroid in each time step n is defined as $error(n) = (\sum_{m=1}^N \|(p_m(n) - \tilde{C}_{V_m^g}(n))\|^2) / \max_{i \in I_M}(error(i))$, where M is the total number of time steps to achieve the optimal deployment. This history of error is plotted against the number of time steps along with the value of the objective function in Figures 3(a) and 3(b) for the same set of parameters as above.

The trajectories of agents with an exponential density distribution having a peak near the center of the space are shown in Figures 4(a) and 4(b) along with the generalized Voronoi partition corresponding to the final position of the agents. A contour plot of density distribution is also shown. It can be observed that more agents are deployed near the peak of density distribution. Figure 4(a) corresponds to agents having different α and leads to a multiplicatively weighted Voronoi partition with values of α shown near the agents' final positions. Figure 4(b) corresponds to homogeneous agents leading to standard Voronoi partition. The corresponding plots showing history of error and value of objective functions can be seen in Figures 5(a) and 5(b). It is evident that the error is reducing and the objective function is getting maximized.

Figures 6(a) and 6(b) show similar results for an exponential density distribution with peak

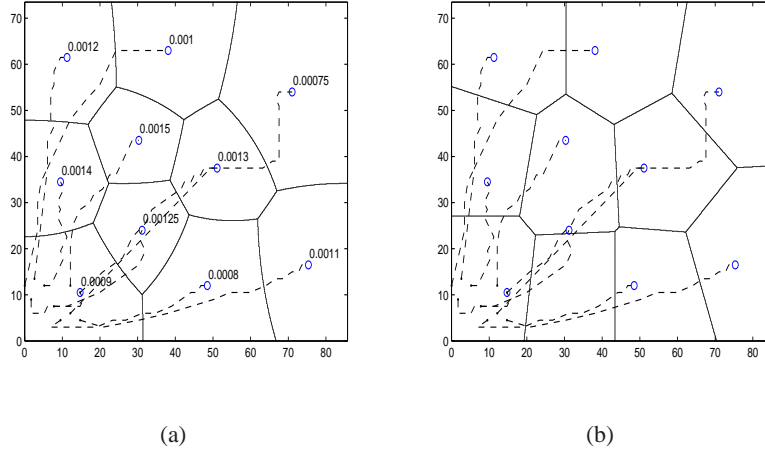


Fig. 2. Trajectories of agents with $f_i(r_i) = -\alpha_i r_i^2$, with uniform density, and a) heterogeneous sensors with different α b) homogeneous sensors, and History of error and value of objective function with $f(r) = -\alpha r^2$, with uniform density.

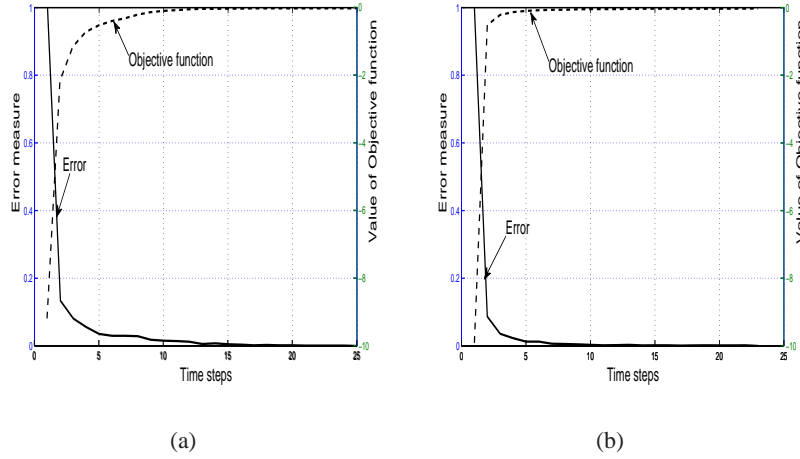


Fig. 3. History of error and value of objective function with $f(r) = -\alpha r^2$, with uniform density, and a) heterogeneous sensors with different α b) homogeneous sensors.

toward the corner of the space. It can be clearly observed in both heterogeneous (Figure 6(a)) and homogeneous (Figure 6(b)) agents move toward the region of maximum density. Figures 7(a) and 7(b) show that the error measure decreases and the objective function is maximized as the agents get deployed.

Next similar results are provided with $f_i(r_i) = k_i e^{-\alpha_i r_i^2}$. Simulations were carried out by either fixing k_i or α_i , or varying both, and with uniform and exponential density distribution. The case of both k_i and α_i fixed is the same as fixing α_i in the previous set of experiments and corresponds to the homogeneous agent case and leads to a standard Voronoi partition. Figures 8,

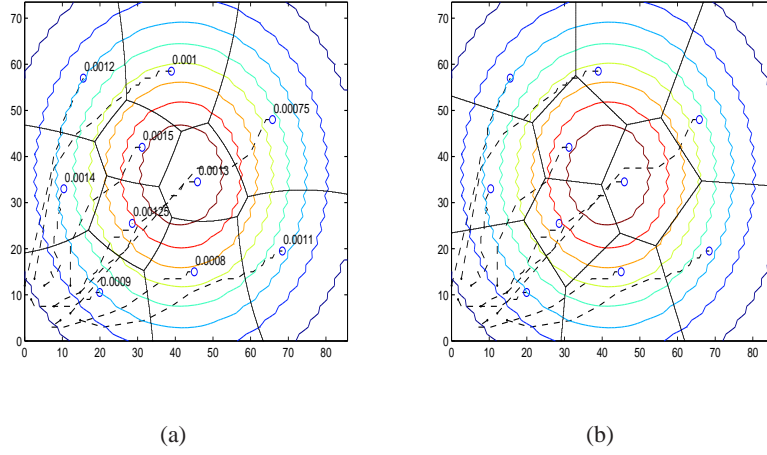


Fig. 4. Trajectories of agents with $f_i(r_i) = -\alpha_i r_i^2$, with exponential density having peak at the center of space, and a) heterogeneous sensors with different α b) homogeneous sensors.

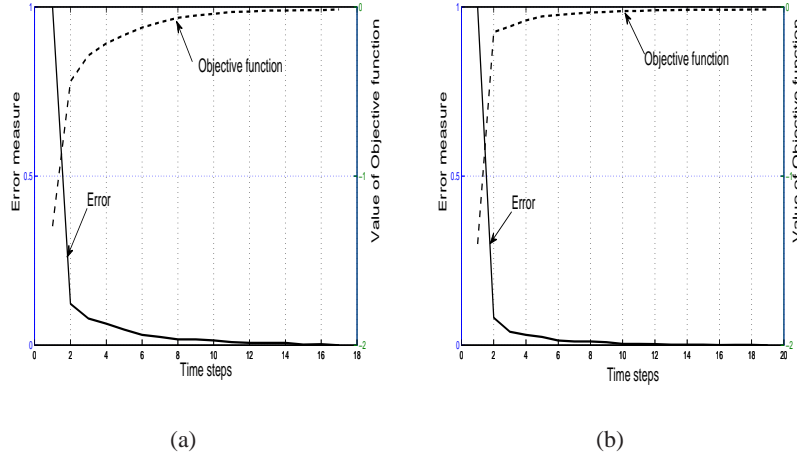


Fig. 5. History of error and value of objective function with $f_i(r_i) = -\alpha_i r_i^2$, with exponential density having peak at the center of space, and a) heterogeneous sensors with different α b) homogeneous sensors.

10, and 12 show the trajectories of agents with exponential density having peak near the center, exponential density having peak near the corner, and an uniform density. Figures 8(a), 10(a), and 12(a) correspond to cases where all the agents have the same α_i , but different k_i . Figures 8(b), 10(b), and 12(b) correspond to case where all the agents have the same k_i and different α_i . Figures 8(c), 10(c), and 12(c) correspond to cases where all the agents have different k_i and α_i . When k_i is fixed, it leads to multiplicatively weighted Voronoi partition, when α_i is fixed it leads to a generalized Voronoi partition with intersection between any two cells being a straight line segment, and when both k_i and α_i vary, it leads to a generalized Voronoi partition. A contour

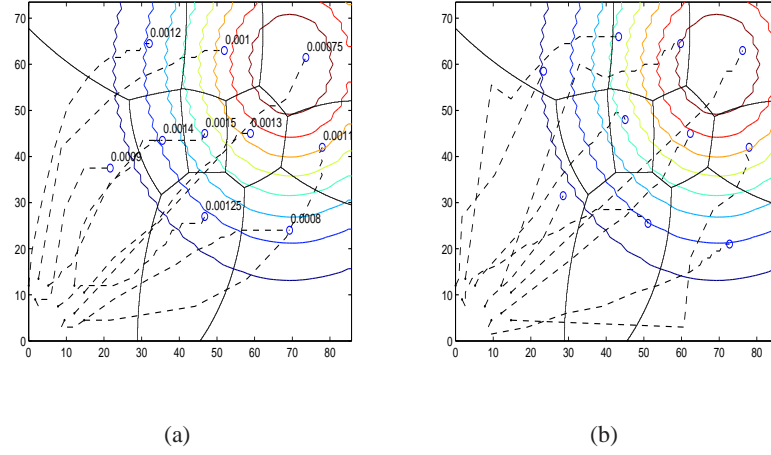


Fig. 6. Trajectories of agents with $f_i(r_i) = -\alpha_i r_i^2$, with exponential density having peak toward the corner of space, and a) heterogeneous sensors with different α b) homogeneous sensors.

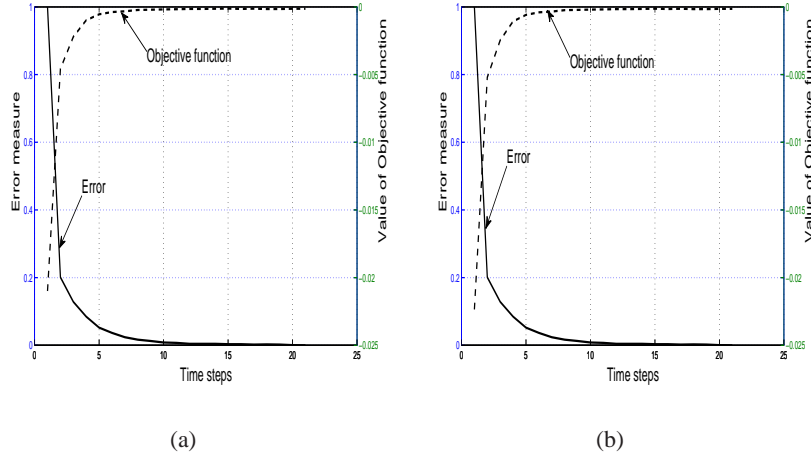


Fig. 7. History of error and value of objective function with $f_i(r_i) = -\alpha_i r_i^2$, with exponential density having peak toward the corner of space, and a) heterogeneous sensors with different α b) homogeneous sensors.

plot is also shown for exponential density cases. It can be observed that the agents move toward the peak of density. As before, dots indicate the starting position of agents and 'o's indicate the final position.

Figures 9, 11, and 13 show the history of error and the objective functions for the corresponding simulations. As noted earlier, in all cases the error reduces and the objective function is maximized.

Next, a set of results are presented with speed and range limits imposed on the agents/sensors. The maximum speed constraint or the constant speed constraints of agents can only make the

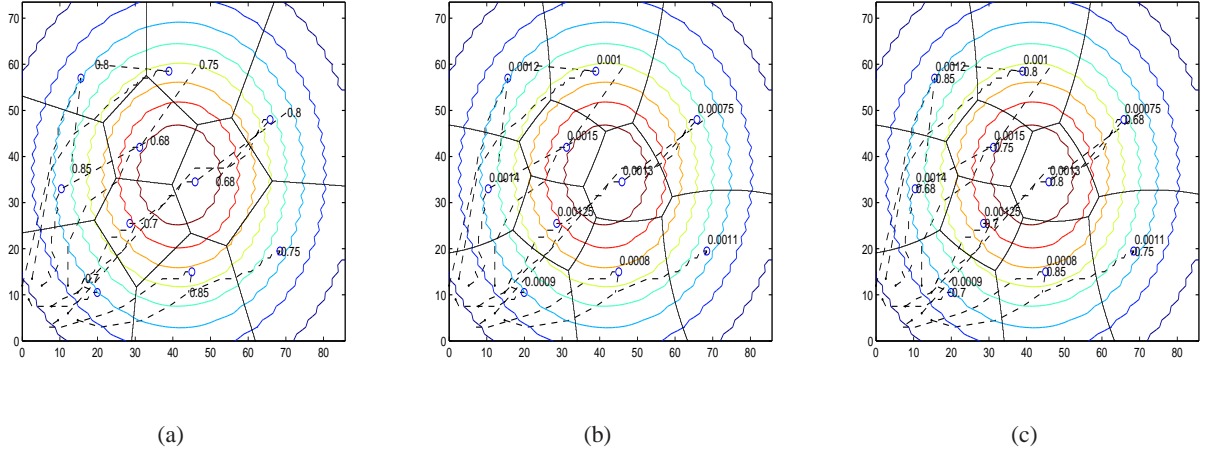


Fig. 8. Trajectories of agents with $f_i(r_i) = k_i e^{\alpha r_i^2}$, with exponential density having peak at the center of space, and a) α fixed and k varying b) α varying and k fixed c) both α and k varying.

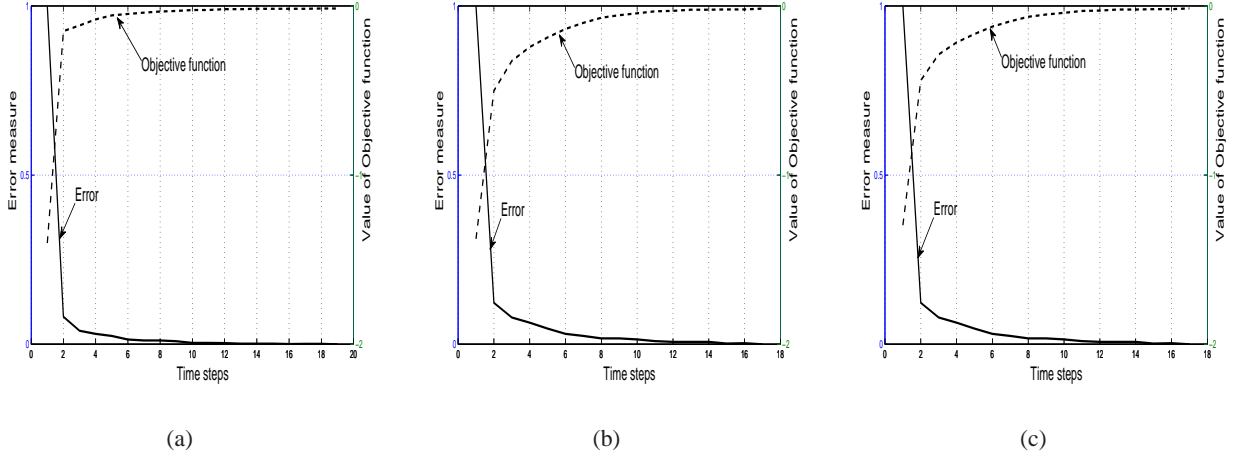


Fig. 9. History of error and value of objective function with $f_i(r_i) = k_i e^{\alpha r_i^2}$, with exponential density having peak at the center of space, and a) α fixed and k varying b) α varying and k fixed c) both α and k varying.

convergence a bit slower depending on the speed limit. Limits on the sensor range has two important implications. Firstly, the space covered is now only $\bigcup_i \bar{B}(p_i, R_i) \subset Q$, which is the part of the space accessible to the agents. This fact is reflected in the objective function (17). Secondly, if the sensor range is too small, each agent will try to move toward the centroid of the area $\bar{B}(p_i, R_i)$, as $V_i^g \cap \bar{B}(p_i, R_i) \rightarrow \bar{B}(p_i, R_i)$. The limit on the range of the i -th sensor is computed as $R(i) = \sqrt{-\ln(C/k(i))/\alpha(i)}$ with cutoff strength $C = 0.05$. If $k = 1$, then $C = 0.05$ corresponds to a cutoff strength of 5%. A speed limit of 25 units is assumed.

The simulation experiments were carried out with node function $f_i(r_i) = e^{\alpha_i r_i^2}$. As in the case

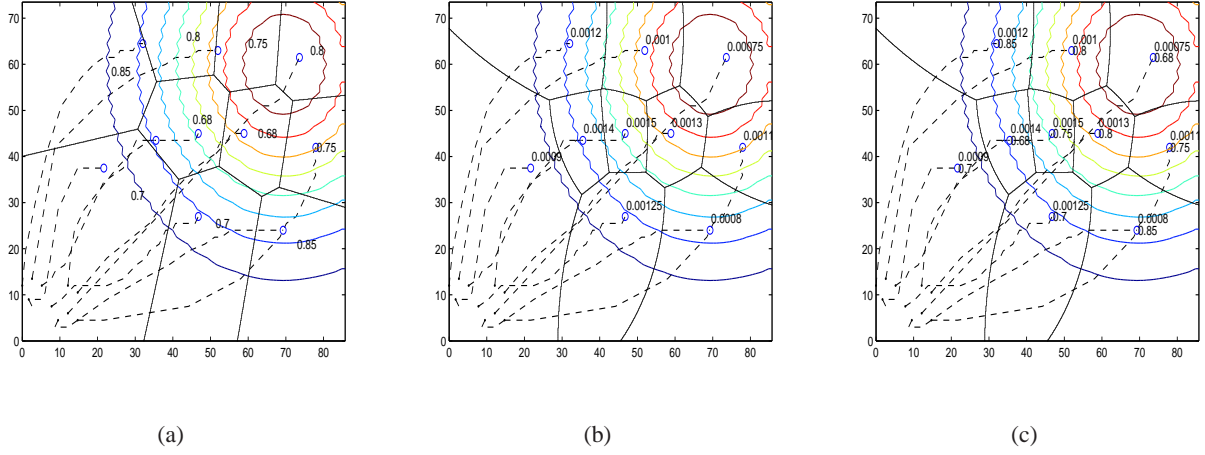


Fig. 10. Trajectories of agents with $f_i(r_i) = k_i e^{\alpha r_i^2}$, with exponential density having peak toward the corner of space, and a) α fixed and k varying b) α varying and k fixed c) both α and k varying.

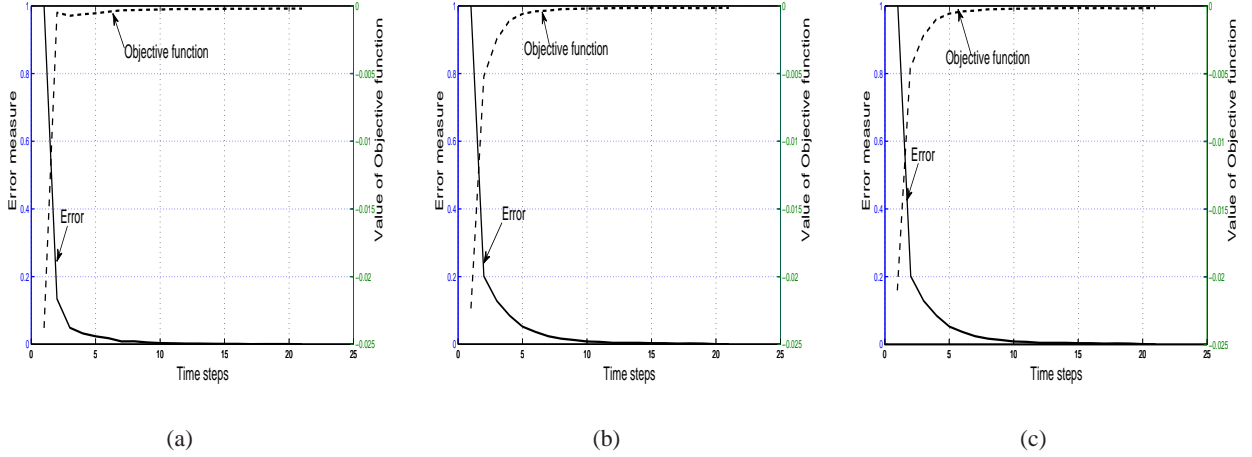


Fig. 11. History of error and value of objective function with $f_i(r_i) = k_i e^{\alpha r_i^2}$, with exponential density having peak toward the corner of space, and a) α fixed and k varying b) α varying and k fixed c) both α and k varying.

of previous simulations, three density distributions, namely, uniform, exponential with peak near the center of the space, and exponential with peak near one of the corners of the space have been used. The case with $k_i = k$, and $\alpha_i = \alpha$, $\forall i \in I_N$ corresponds to a homogeneous multi-agent system. Along with the generalized Voronoi cells corresponding to the final configuration of agents, part of $\bar{B}(p_i, R_i)$ within the corresponding cells are shown which show the region $\bigcup_i \bar{B}(p_i, R_i) \subset Q$.

Figure 14 shows trajectories of agents when the density distribution is exponential with the peak near the center. As before, dots show the starting location of agents and ‘o’s show

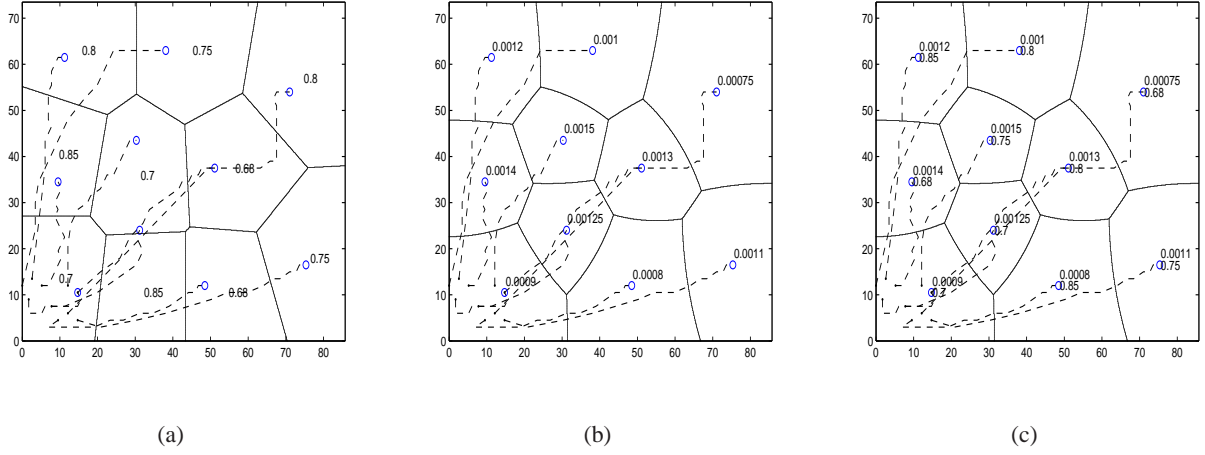


Fig. 12. Trajectories of agents with $f_i(r_i) = k_i e^{\alpha r_i^2}$, with uniform density, and a) α fixed and k varying b) α varying and k fixed c) both α and k varying.

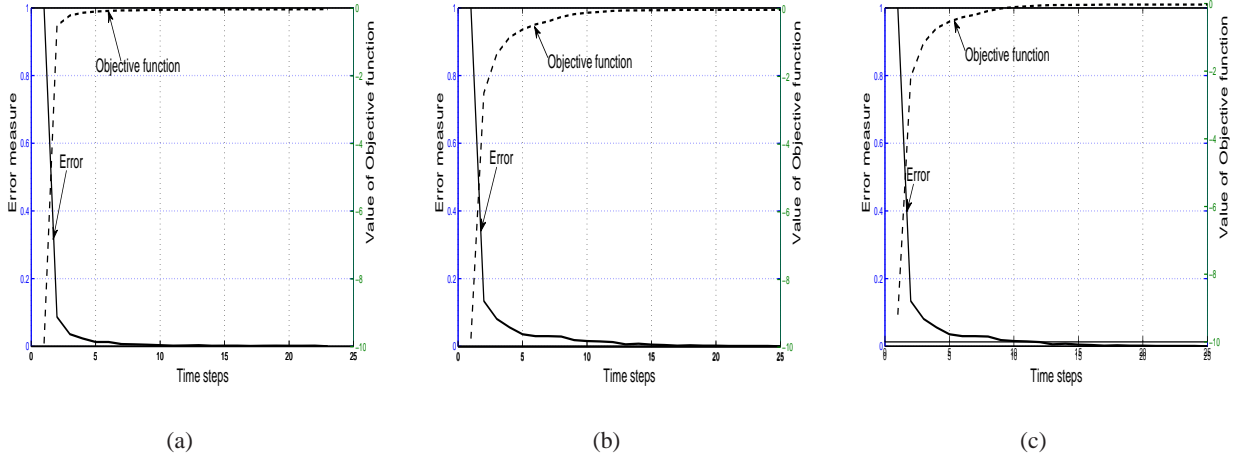


Fig. 13. History of error and value of objective function with $f_i(r_i) = k_i e^{\alpha r_i^2}$, with uniform density, and a) α fixed and k varying b) α varying and k fixed c) both α and k varying.

the final configuration. Along with the generalized Voronoi cells corresponding to final agent configuration, the circular arcs around a few of the agents represent the part of $\bar{B}(p_i, R_i)$ which is within V_i^g showing the region $\bigcup_i \bar{B}(p_i, R_i) \subset Q$.

The size of the hexagonal grid plays an important role in convergence of the discretized implementation. This issue becomes more critical with limit on the sensor range. The simulation results presented in this paper are only to illustrate the optimal deployment strategy. Finer issues on discretizing and optimal selection of the node functions are beyond the scope of the present work.

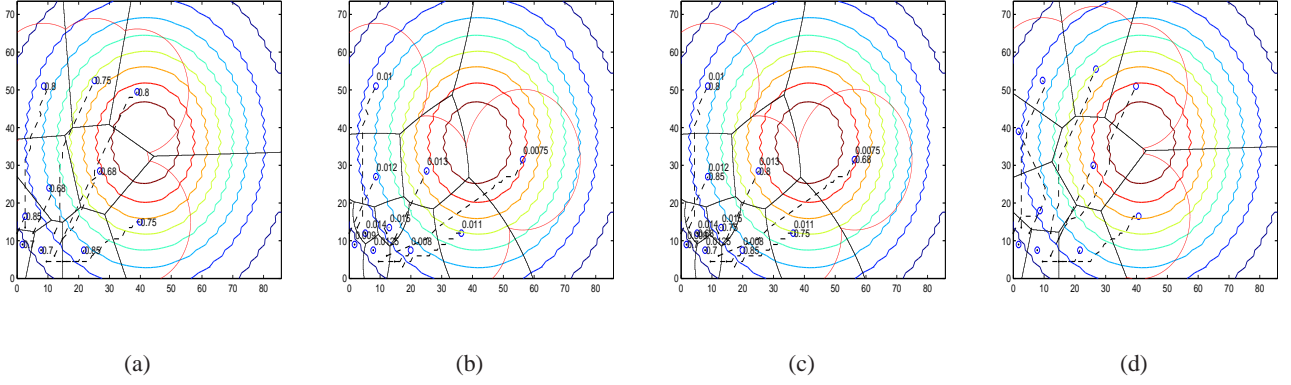


Fig. 14. Trajectories of agents with sensor range limit and agent speed limit of 25 units, and with node functions $f_i(r_i) = k_i e^{\alpha r_i^2}$, with exponential density having peak at the center of space, and a) α fixed and k varying b) α varying and k fixed c) both α and k varying, and d) homogenous sensors.

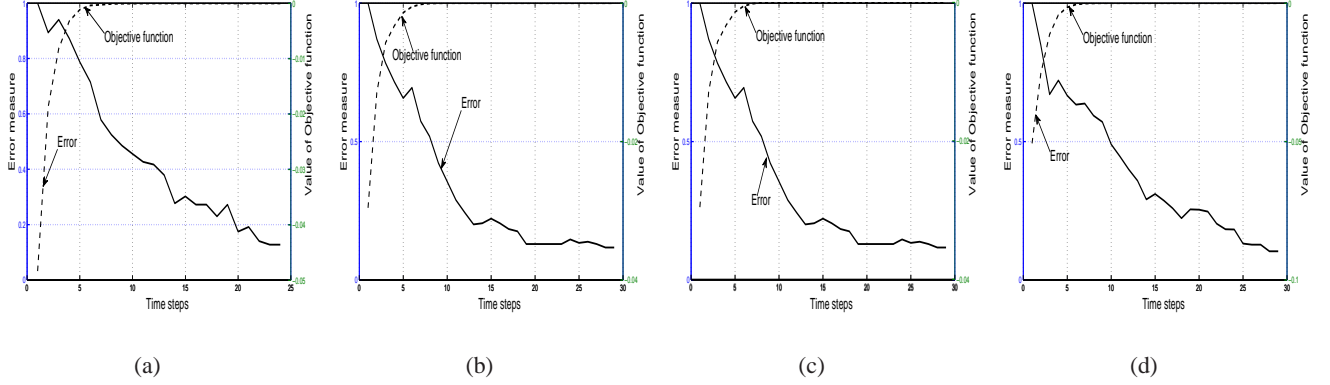


Fig. 15. History of error and value of objective function with sensor range limit and agent speed limit of 25 units, and with node functions $f_i(r_i) = k_i e^{\alpha r_i^2}$, with exponential density having peak at the center of space, and a) α fixed and k varying b) α varying and k fixed c) both α and k varying, and d) homogenous sensors.

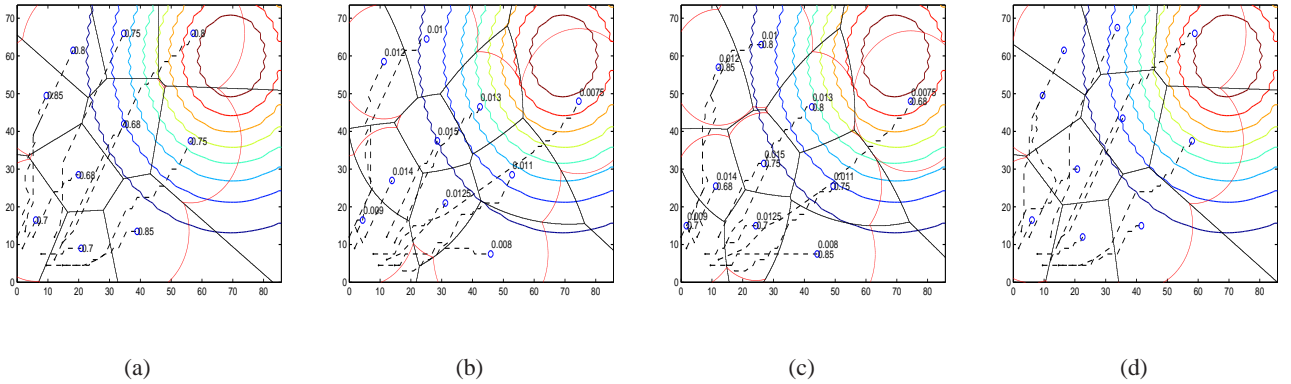


Fig. 16. Trajectories of agents of agents with a sensor range limit and agent speed limit of 25 units, and node functions $f_i(r_i) = k_i e^{\alpha r_i^2}$, with exponential density having peak toward the corner of space, and a) α fixed and k varying b) α varying and k fixed c) both α and k varying and d) homogeneous sensors.

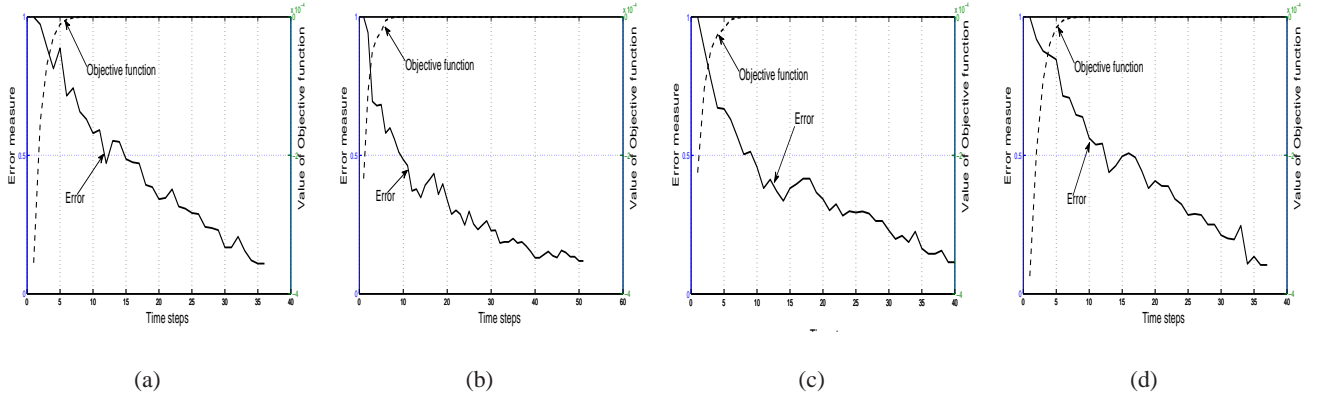


Fig. 17. History of error and value of objective function with a sensor range limit and agent speed limit of 25 units, and node functions $f_i(r_i) = k_i e^{\alpha r_i^2}$, with exponential density having peak toward the corner of space, and a) α fixed and k varying b) α varying and k fixed c) both α and k varying and d) homogeneous sensors.

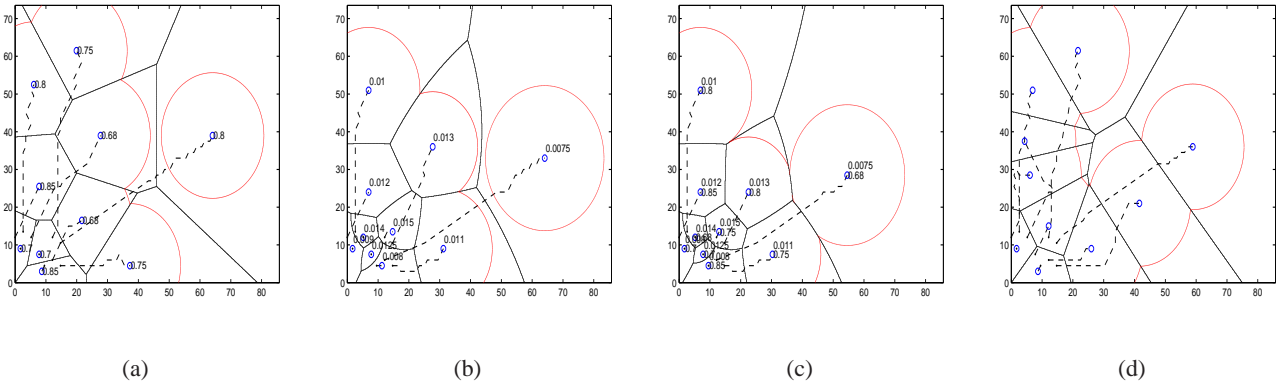


Fig. 18. Trajectories of agents with a sensor range limit and agent speed limit of 25 units, and node functions $f_i(r_i) = k_i e^{\alpha r_i^2}$, with uniform density, and a) α fixed and k varying b) α varying and k fixed c) both α and k varying and d) homogeneous sensors.

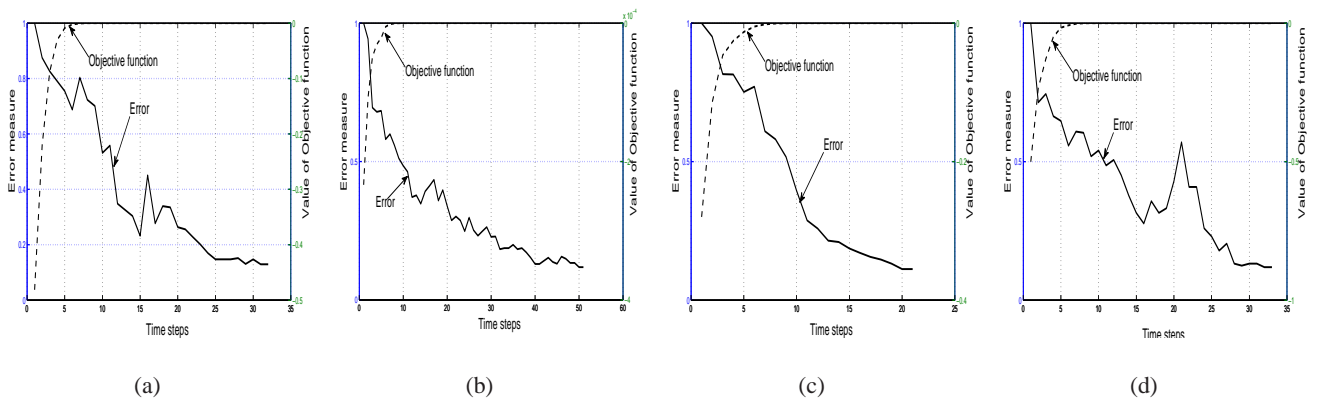


Fig. 19. History of error and value of objective function with a sensor range limit and agent speed limit of 25 units, and node functions $f_i(r_i) = k_i e^{\alpha r_i^2}$, with uniform density, and a) α fixed and k varying b) α varying and k fixed c) both α and k varying and d) homogeneous sensors.

VII. CONCLUSIONS

A generalization of Voronoi partition has been proposed and the standard Voronoi decomposition and its variations are shown to be special cases of this generalization. A heterogeneous spatially distributed locational optimization problem has been formulated and solved using the proposed partitioning scheme and the centroidal Voronoi configuration is shown to be the optimal deployment of the limited range sensors with heterogeneous capabilities. Illustrative simulation results are provided to support the theoretical results.

The generalization of Voronoi partition and the heterogeneous locational optimization techniques can be applied to a wide variety of problems, such as spraying insecticides, painting by multiple robots with heterogeneous sprayers, and many others. The heterogeneous locational optimization problems can find applications outside robotics field. One such problem is of deciding on optimal location for public facilities. Take for example a problem of deciding on optimal location for N new hospitals. The heterogeneity comes from the fact that all hospitals may not have same capacity, and a suitable node function f_i can be used to model this. The density distribution of the population needing the hospital can be modeled as $\phi(q)$. Heterogeneity can also be used as a tunable parameter.

The generalization of Voronoi partition presented also provides new challenges for developing efficient algorithms for computations related to the generalized Voronoi partition, and characterizing its properties.

ACKNOWLEDGEMENTS

This work was partly supported by Indian National Academy of Engineering (INAE) fellowship under teacher mentoring program.

APPENDIX

APPENDIX: CONTINUITY OF GENERALIZED VORONOI PARTITION

A proof on the continuity of the generalized Voronoi partition is provided here for. The treatment provided here is kept informal, but discusses major steps for a more elaborate mathematical proof, which is beyond the scope of this paper.

Consider a partition $\mathcal{W}(\mathcal{P}) = \{W_i(\mathcal{P})\}, i \in I_N$ of $Q \subset \mathbb{R}^2$ with $\mathcal{P} = \{p_1, p_2, \dots, p_N\}$, $p_i \in Q$. Let $\partial W_i(\mathcal{P})$ be the bounding (closed) curve of cell W_i , parameterized by a parameter

$u_i(\mathcal{P}) \in [0, 1]$. The partition $\mathcal{W}(\mathcal{P})$ is said to be continuous in \mathcal{P} if and only if each of the $u_i(\mathcal{P})$ is continuous in \mathcal{P} . That is, the cell boundaries move smoothly with configuration of sites \mathcal{P} . This is an important property needed for proving the stability and convergence of the agent motion under the influence of the proposed control law using LaSalle's invariance principle. This understanding of continuity of a partition can be extended to a general d -dimensional Euclidean space. Now, in \mathbb{R}^d ∂W_i are hypersurfaces in d -dimensional Euclidean space and u_i are vector valued functions of dimension $d - 1$. Continuity of u_i^j , the j -th component of u_i with \mathcal{P} for each $i \in I_N$ and $j \in I_{d-1}$ ensures the continuity of $\mathcal{W}(\mathcal{P})$ when $Q \subset \mathbb{R}^d$.

Now consider the continuity of standard Voronoi partition. It is well known, that as long as $p_i \neq p_j$, whenever $i \neq j$, $\mathcal{V}(\mathcal{P})$, the standard Voronoi partition is continuous in \mathcal{P} . This continuity is due to continuity of the Euclidean distance. It is interesting to see what happens when $p_i = p_j$ for some $i \neq j$. Consider $i \neq j$ and let $p_i(0) \neq p_j(0)$. Now, V_i and V_j are distinct sets such that $V_i \cap V_j$ is either \emptyset or is the common boundary between them, which is a straight line segment of the perpendicular bisector of the line joining p_i and p_j . Let $V_i \cap V_j \neq \emptyset$, that is, the agents i and j are Voronoi neighbors, and agent i is stationary while agent j is moving toward i . This causes V_i to shrink and V_j to expand as the common boundary between them moves closer to p_i . But, when $p_j(t) = p_i(t)$, $V_i(t) = V_j(t) = V_i(0) \cup V_j(0)$, which is a sudden jump, and boundaries of both V_i and V_j jump, leading to discontinuity. Thus, $\mathcal{V}(\mathcal{P})$ is discontinuous whenever there is a transition between $p_i \neq p_j$ and $p_i = p_j$, for some $i \neq j$. Similar discontinuity as in standard Voronoi partition with \mathcal{P} can occur in the case of generalized Voronoi partition, whenever p_i and p_j are Voronoi neighbors and $f_i = f_j$. This is illustrated in Figure 20. The line segment separating V_1^g and V_2^g disappears when $p_1 = p_2$ and the corresponding Voronoi cells jump in their size. In fact V_1^g and V_2^g jump to $V_1^g \cap V_2^g$, and the common boundary between V_1^g and V_2^g jumps to the boundary of $V_1^g \cap V_2^g$.

In case of standard Voronoi partition, if $p_i(0) \neq p_j(0)$, whenever $i \neq j$, the control law making the agents move toward the centroids will ensure that $p_i(t) \neq p_j(t)$, whenever $i \neq j$, $\forall t > 0$. It should also be noted that if two agents are together to start with, that is, $p_i(0) = p_j(0)$, whenever $i \neq j$, then the control law will ensure that they are always together. This is because of the fact that V_i is convex and hence $\tilde{C}_{V_i} \in V_i$, $\forall i \in I_N$. This is not always true in case of the generalized Voronoi partition. Thus, the issue of continuity of generalized Voronoi partition is a bit more involved.

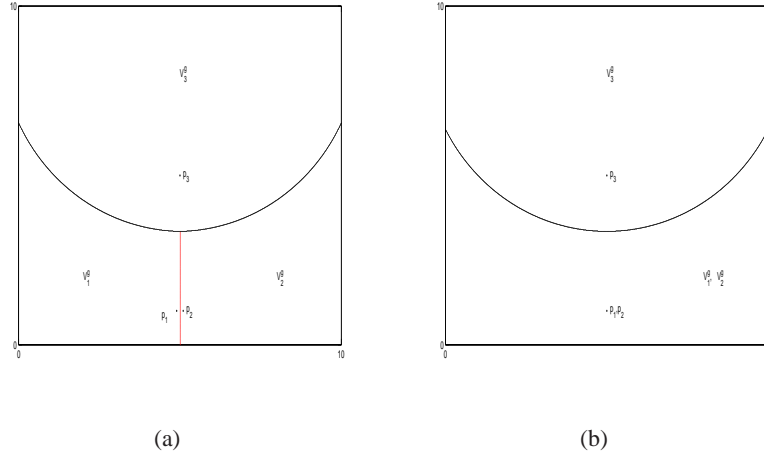


Fig. 20. Illustration of discontinuity of Voronoi partition at $p_1 = p_2$ when $f_1 = f_2$. The straight line segment separating V_1^g and V_2^g suddenly disappears when two points p_1 and p_2 merge.

Condition A. There is no transition from $\mathcal{P}(t)$ to $\mathcal{P}(t')$, such that $p_i(t) \neq p_j(t)$ and $p_i(t') = p_j(t')$, for all pairs (i, j) , $i \neq j$, $i, j \in I_N$, and $f_i = f_j$.

As discussed earlier, violation of the condition A can cause discontinuity in the generalized Voronoi partition.

Lemma A1: The generalized Voronoi partition depends continuously on \mathcal{P} if condition A is satisfied.

Outline of the proof: Let us consider any two agents i and j which are Voronoi neighbors; take up three distinct and exhaustive cases, and prove the continuity for each of them.

Case i) No two node functions are identical, that is, $(f_i - f_j) \neq 0$, whenever $i \neq j$, and $V_i^g \neq \emptyset$, $\forall i \in I_N$. $\forall \mathcal{P}$.

All the points $q \in Q$ on the boundary common to V_i^g and V_j^g is given by $\{q \in Q | f_i(\|p_i - q\|) = f_j(\|p_j - q\|)\}$, that is, the intersection of the corresponding node functions. Let the j -th agent move by a small distance dp . This makes a point $q \in Q$, on the common boundary between V_i and V_j move by a distance, say dx . Now, as the node functions are strictly decreasing and are continuous, it is easy to see that $dx \rightarrow 0$ as $dp \rightarrow 0$. This is true for any two i and j , and any q on the common boundary between V_i^g and V_j^g . Thus, the generalized Voronoi partition depends continuously on \mathcal{P} . Note that it is easy to verify that $p_i = p_j$ for $i \neq j$ does not lead to discontinuity in this case.

Case ii) No two node functions are identical, that is, $(f_i - f_j) \neq 0$, whenever $i \neq j$, and \mathcal{P} is such that $V_i^g = \emptyset$ for some $i \in I_N$.

Let both V_i^g and V_j^g be non null sets, and $V_i^g \subset V_j^g$ for some \mathcal{P} . Now with evolution of \mathcal{P} in time, let $V_i^g = \emptyset$ for some $\mathcal{P}' = \mathcal{P} + \delta\mathcal{P}$. The quantity $\int_{V_i^g} dQ$, and the common boundary vanish gradually to zero as the agent configuration changes from \mathcal{P} to \mathcal{P}' . Further, there is no jump in the boundary or size of the (generalized) Voronoi cell, or in the common boundary as in the case of standard Voronoi cell when there is a transition from $p_i \neq p_j$ to $p_i = p_j$.

Case iii). For some $i \neq j$, $f_i = f_j$. In this case, the common boundary between V_i^g and V_j^g is a segment of the perpendicular bisector of line joining p_i and p_j . As in the case of standard Voronoi diagram, if agents i and j are neighbors and there is a transition from $p_i \neq p_j$ to $p_i = p_j$, the $\mathcal{V}^g(\mathcal{P})$ will have discontinuity. However, if condition A is satisfied, such a discontinuity will not occur.

Thus, as long as the condition A is satisfied, the generalized Voronoi partition depends continuously on \mathcal{P} . \square

Lemma A2: The control law (12) ensures that condition A is satisfied for all \mathcal{P} if $p_i(0) \neq p_j(0)$ for all pairs $(i, j), i, j \in I_N, i \neq j$, for which $f_i = f_j$.

Proof. Condition A can be violated only for pair i, j for which $f_i = f_j$. As $p_i(0) \neq p_j(0)$, condition A will be violated if at some time t , $p_i(t) = p_j(t)$. Now $\tilde{C}_{V_i^g}$ will lie within the half plane $\{q \in Q \mid \|q - p_i\| < \|q - p_j\|\}$ and hence the control law cannot make the agent i cross the common boundary between i and j . Similarly, agent j too cannot cross the boundary. Hence, if $p_i(0) \neq p_j(0)$, then $p_i(t) \neq p_j(t)$ for any $t \in \mathbb{R}$. Thus, the condition A cannot be violated. \square

Theorem A3: If $\mathcal{P}(0)$ is such that $p_i(0) \neq p_j(0)$ for all pairs $(i, j), i, j \in I_N, i \neq j$, for which $f_i = f_j$, and the agents move according to the control law (12), then the generalized Voronoi partition depends continuously on \mathcal{P} .

Proof. The proof follows from Lemmas A1 and A2. \square

REFERENCES

- [1] R.W. Beard, J. Lawton, and F.Y. Hadaegh, A coordination architecture for spacecraft formation control, *IEEE Transactions on Control Systems Technology*, vol. 9, issue 6, 2001, pp. 777 - 790.
- [2] T. Keviczky, F. Borrelli, K. Fregene, D. Godbole, and G.J. Balas, Decentralized receding horizon control and coordination of autonomous vehicle formations, *IEEE Transactions on Control Systems Technology*, vol. 16, issue 1, 2008, pp. 19 - 33.

- [3] A. Macwan, G. Nejat, and B. Benhabib, Target-motion prediction for robotic search and rescue in wilderness environments, *IEEE Transactions on Systems, Man, and Cybernetics, Part B: Cybernetics*, to appear.
- [4] Y. Yao, C-H. Chen, B. Abidi, D. Page, A. Koschan, and M. Abidi, Can you see me now? sensor positioning for automated and persistent surveillance, *IEEE Transactions on Systems, Man, and Cybernetics, Part B: Cybernetics*, vol. 40, issue 1, 2010, pp. 101 - 115.
- [5] A.E. Gil, K.M. Passino, and J.B. Cruz, Stable cooperative surveillance with information flow constraints, *IEEE Transactions on Control Systems Technology*, vol. 16, issue 5, 2008, pp. 856 - 868.
- [6] M.E. Campbell, W.W. Whitacre, Cooperative tracking using vision measurements on seascan UAVs, *IEEE Transactions on Control Systems Technology*, vol. 15, issue 4, 2007, pp. 613 - 626.
- [7] D. Gu, A game theory approach to target tracking in sensor networks, *IEEE Transactions on Systems, Man, and Cybernetics, Part B: Cybernetics*, vol 41, issue 1, pp. 2-13.
- [8] Cheng-Ming Huang Li-Chen Fu, Multitarget visual tracking based effective surveillance with cooperation of multiple active cameras, *IEEE Transactions on Systems, Man, and Cybernetics, Part B: Cybernetics*, vol. 41, issue 1, Feb 2011, pp. 2354-247.
- [9] C. G. Cassandras and W. Li, Sensor networks and cooperative control, *European J. Control*, vol. 11, no. 4-5, 2005, pp. 436-463.
- [10] W. Li and C.G. Cassandras, Distributive cooperative coverage control of mobile sensing networks, *Proc. IEEE Conference on Decision and Control, and the European Control Conference*, Seville, Spain, December 2005, pp. 2542-2547.
- [11] Y. Zou and K. Chakrabarty, Sensor deployment and target localization baesd on virtual forces, *Proc. of IEEE INFOCOM*, 2003, pp. 1293-1303.
- [12] I.I. Hussein and D.M. Stipanovic, Effective coverage control for mobile sensor networks with guaranteed collision avoidance, *IEEE Transactions on Control Systems Technology*, vol. 15, issue 4, July 2007, pp. 642-657.
- [13] K. Chakrabarty, S.S. Iyengar, H. Qi, Grid coverage for surveillance and target location in distributed sensor networks, *IEEE Transactions on Computers*, vol 51, no. 12, December 2002, pp. 1488-1453.
- [14] A.T. Murray, K. Kim, J.W. Davis, R. Machiraju, and R. Parent, Coverage optimization to support security monitoring, *Computers, Environment and Urban Systems* , vol. 31, 2007, pp. 133-147.
- [15] V. Akbarzadeh, A. Hung-Ren Ko, C. Gagn and M. Parizeau, Topography-aware sensor deployment optimization with CMA-ES, *Parallel Problem Solving From Nature - PPSN XI, Lecture Notes in Computer Science*, vol. 6239, 2011, pp. 141-150.
- [16] Z. Drezner, *Facility Location: A Survey of Applications and Methods*, New York, NY: Springer, 1995.
- [17] A. Okabe and A. Suzuki, Locational optimization problems solved through Voronoi diagrams, *Eurpean Journal of Operations Research*, vol. 98, no. 3, 1997, pp. 445-456.
- [18] Q. Du, V. Faber and M. Gunzburger, Centroidal Voronoi tessellations: applications and algorithms, *SIAM Review*, vol. 41, no. 4, 1999, pp. 637-676.
- [19] Guruprasad K. R. and D. Ghose, Automated multi-agent search using centroidal voronoi configuration, *IEEE Tansactions on Automation Science and Engineering*, vol. 8, issue 2, April 2011, pp. 420 - 423.
- [20] S. Salapaka, A. Khalak, and M.A. Dahleh, Constraints on locational optimization problems, *Proc of the 42nd IEEE Conference on Decision and Control*, Maui, Hawaii, USA, December, 2003, pp. 1741-1746.
- [21] J. Cortes, S. Martinez, and F. Bullo, Spatially-distributed coverage optimization and control with limited-range interactions, *ESAIM: Control, Optimization and Calculus of Variations*, vol. 11, no. 4, 2005, pp. 691-719.

- [22] T.M. Cavalier, W.A. Connera, E.-del Castilloa and S.I. Brown, A heuristic algorithm for minimax sensor location in the plane, *European Journal of Operational Research*, vol. 183, issue 1, November 2007, pp. 42-55.
- [23] L.C.A. Pimenta, V. Kumar, R.C. Mesquita, and A.S. Pereira, Sensing and coverage for a network of heterogeneous robots, *Proceedings of IEEE Conference on Decision and Control*, Cancun, December 2008, pp 3947 - 3952 .
- [24] A. Kwok and S. Martínez, Deployment algorithms for a power-constrained mobile sensor network, *International Journal of Robust and Nonlinear Control*, vol. 20, issue 7, 2002, pp. 745-763.
- [25] M. Pavone, A. Arsie, E. Frazzoli, and F. Bullo, Equitable partitioning policies for robotic networks, *Proc of the 2009 IEEE International Conference on Robotics and Automation*, Kobe, Japan, 2009, pp. 3979-3984.
- [26] K.R. Guruprasad and D. Ghose, Heterogeneous sensor based Voronoi decomposition for spatially distributed limited range locational optimization, in *Voronoi's Impact on Modern Science, Book 4, vol. 2, Proceedings of 5th Annual International Symposium on Voronoi Diagrams (ISVD 2008)*, Kiev, Ukraine, September 2008, pp. 78-87.
- [27] A. Gusrialdi, S. Hirche, T. Hatanaka, and M. Fujita, Voronoi based coverage control with anisotropic sensors, *Proceedings the American Control Conference*, 2008, pp. 736-741.
- [28] K. Laventall and J. Cortés, Coverage control by multi-robot networks with limited-range anisotropic sensory, *International Journal of Control*, vol. 82, issue 6, June 2009, pp. 1113-1121.
- [29] M. Zhong and C.G. Casaandras, Distributed coverage control in sensor network environments with polygonal obstacles, *Proc of the 17th IFAC world congress*, July 2008, pp. 4162-4167.
- [30] C.H. Caicedo-núñez and M. Žefran, A coverage algorithm for a class of non-convex regions, *Proc of the 47th IEEE Conference on Decision and Control*, Mexico, December 2008, pp. 4244-4249.
- [31] G. Voronoi, Nouvelles applications des paramtres continus la thorie des formes quadratiques, *Journal fr die Reine und Angewandte Mathematik*, vol. 133, 1907, pp. 97-178.
- [32] G.L. Dirichlet, ber die Reduktion der positiven quadratischen Formen mit drei unbestimmten ganzen Zahlen, *Journal fr die Reine und Angewandte Mathematik*, vol. 40, 1850, pp. 209-227.
- [33] F. Aurenhammer, Voronoi diagrams - A survey of a fundamental geometric data structure, *ACM Computing Surveys*, vol 23, no. 3, 1991, pp. 345-405.
- [34] P.A. Arbelález and L.D. Cohen, Generalized Voronoi tessellations for vector-valued image segmentation, *International Journal of Computer Vision, Special Issue on Geometrical, Variational and Level Sets Methods in Computer Vision*, vol. 69, no. 1, 2006, pp.119-126.
- [35] H. Edelsbrunner and R. Seidel, Voronoi diagrams and arrangements, *Discrete Comput. Geom.*, vol 1, 1986, pp. 25-44.
- [36] S.G. Krantz and H.R. Parks, *A Primer of Real Analytic Functions* (2nd edn.), Birkhäuser Advanced Texts, Basler Lehbücher, 2002.
- [37] P.K. Kundu and I.M. Cohen, *Fluid Mechanics* (2nd edition), Academic Press, 2002.
- [38] H.J. Marquez, *Nonlinear Control Systems - Analysis and Design*, John Wiley & Sons, Inc., 2003.
- [39] F. Blanchini, Set invariance in control, *Automatica*, vol. 35, 1999, pp. 1747-1767.